Drug Design, Development and Therapy Dovepress

Open Access Full Text Article ORIGINAL RESEARCH

Integrating Metabolomics, Histopathology, and Cardiac Marker Analysis to Assess Valsartan's Efficacy in Mitigating Dasatinib-Induced Cardiac Toxicity in Sprague-Dawley Rats

Khalid Alhazzani[1], Hanan Mohammed[1], Mohammad M Algahtani[1], Khaldoon Aljerian[2], Ali Alhoshani[1], Homood M As Sobeai[1], Syed Rizwan Ahamad[3], Moureq R Alotaibi[1], Abdullah S Alhamed[1], Fawaz Alasmari[1], Mohammed Alqinyah[1], Hussain N Alhamami[1], Ahmed Z Alanazi[1]

[1]Department of Pharmacology & Toxicology, College of Pharmacy, King Saud University, Riyadh, Saudi Arabia; [2]Department of Pathology, College of Medicine, King Saud University, Riyadh, Saudi Arabia; [3]Department of Pharmaceutical Chemistry, College of Pharmacy, King Saud University, Riyadh, Saudi Arabia

Correspondence: Ahmed Z Alanazi, Department of Pharmacology & Toxicology, College of Pharmacy, King Saud University, Riyadh, 11451, Saudi Arabia, Email azalanazi@ksu.edu.sa

Background: Dasatinib (DASA) is associated with cardiotoxic effects, posing risks to patients. Valsartan (VAL) may offer protective benefits against these effects. This study evaluates the impact of DASA, VAL, and their combination on cardiac health.

Methods: Wistar rats were treated with DASA, VAL, and a combination of VAL and DASA intraperitoneally every other day for 14 days. Body weight and survival rates were monitored. Serum levels of cardiac biomarkers (CPK, LDH, AST) were analyzed. Histopathological and immunohistochemical analyses assessed myocardial architecture and apoptosis-related protein expression. Metabolomic profiling was conducted using GC-MS to identify metabolic changes across treatment groups.

Results: The DASA group experienced significant weight loss and a 50% mortality rate, while the combination group had no mortality. Cardiac biomarkers like CPK, LDH, and AST were elevated in the DASA group but significantly reduced in the VAL + DASA group. Histopathological examination showed significant myocardial injury in the DASA group, with improved cardiac tissue morphology in the combination group. Immunohistochemical analysis revealed altered expression of apoptosis-related proteins, including caspase-3 and BCL-2, with improved levels in the combination group compared to DASA alone. Metabolomic profiling identified significant metabolic shifts, with 15 metabolites differentiating the treatment groups, and the VAL + DASA group mitigated the metabolic disturbances caused by DASA.

Conclusion: The study suggesting VAL's potential therapeutic role in managing DASA-induced cardiac toxicity. The combination of VAL with DASA not only improved survival rates and reduced cardiac biomarker levels but also preserved myocardial architecture and normalized metabolic profiles. These findings highlight the importance of integrated approaches in evaluating drug efficacy and suggest VAL as a promising candidate for protecting cardiac function in preclinical models of DASA therapy.

Keywords: cardiac toxicity, dasatinib, valsartan, metabolomics, histopathology

Introduction

Cardiovascular disease remains the leading cause of mortality among long-term cancer survivors, a demographic that continues to grow despite the advances in cancer treatment.[1] Among the various treatments, targeted chemotherapeutic agents, particularly small-molecule tyrosine kinase inhibitors (TKIs), have been pivotal in improving cancer outcomes. However, these agents are associated with toxic side effects. Despite their design to selectively target cancer cells and minimize collateral damage to healthy cells, TKIs have been implicated in the development of cardiomyopathies.[2] The

Received: 20 September 2024
Accepted: 29 November 2024
Published: 5 December 2024

cardiotoxic effects of TKIs, including hypertrophy, heart failure, and myocardial infarction, pose significant challenges in the management of cancer patients.[3]

Dasatinib (DASA), an oral TKI, has shown substantial efficacy in targeting BCR-ABL, Src family kinases, c-Kit, and platelet-derived growth factor receptors, making it a valuable treatment option for certain leukemias and solid tumors. Specifically, DASA is approved for use in chronic lymphocytic leukemia (CLL) patients who are intolerant or refractory to imatinib, as well as in Philadelphia chromosome-positive acute lymphoblastic leukemia (Ph+ ALL) patients.[4,5] Despite its therapeutic benefits, DASA is associated with significant adverse effects, notably cardiotoxicity. The mechanisms driving DASA-induced cardiotoxicity are not fully understood, but current research points to the involvement of apoptosis induction, inhibition of pro-survival pathways, and other cellular mechanisms.[6,7]

It is crucial to explore cardioprotective drugs that can mitigate the cardiotoxicity associated with DASA. Valsartan (VAL), an angiotensin-receptor blocker, has demonstrated protective effects against cardiovascular diseases and is known for its antihypertensive properties.[8] VAL's ability to selectively block the angiotensin II receptor type 1 is associated with its anti-oxidative, anti-apoptotic, and anti-inflammatory effects, which are beneficial in mitigating cardiovascular damage.[8,9] Furthermore, clinical studies have indicated that VAL may offer cardioprotective benefits in the context of chemotherapy-induced cardiotoxicity.[9–11]

Metabolomics, which involves the study of metabolites in biological samples, can provide valuable insights into the pathophysiological conditions.[12,13] This approach, particularly using gas chromatography-mass spectrometry (GC-MS), allows for the qualitative and quantitative analysis of various metabolites, including amino acids, fatty acids, carbohydrates, nucleosides, and vitamins.[14] By employing metabolomics, we can better understand changes in endogenous metabolites before and after exposure to DASA, thereby elucidating the metabolic shifts associated with cardiotoxicity and the impact of VAL.[15] Therefore, this study aims to assess the protective effect of VAL against DASA-induced cardiotoxicity through histopathology, cardiac biomarkers, and metabolomics profiling. By utilizing metabolomics techniques, this research seeks to shed light on the underlying mechanisms and explore potential therapeutic strategies to minimize the cardiotoxic effects of DASA.

Methods and Materials

Drugs and Chemicals

DASA and VAL were acquired from MedChemExpress (New Jersey, USA; HY-10181 and HY-18204, respectively). Aspartate aminotransferase (AST), lactate dehydrogenase (LDH), and creatine phosphokinase (CPK) measurements were performed using reagents provided by Medical Laboratories Ltd. (Riyadh, Saudi Arabia; EK245084, EK720752, and EK721722, respectively). Primary monoclonal antibodies targeting p53, BCL-2, BAX, and p62 were obtained from Cell Signaling Technology (Massachusetts, USA; 2527, 15071, and 14796, respectively). Secondary antibodies were obtained from Cell Signaling Technology (8114, 8125).

Animals

Male Sprague-Dawley rats weighing 350 ± 20 g were obtained from the Animal Care Center, College of Pharmacy, King Saud University, Riyadh, Saudi Arabia, for the experimental procedures. We selected rats in this weight range because they are approximately 10–12 weeks old, representing healthy young adults.[16] At this stage, the rats are mature but not at risk for age-related or obesity-related heart issues, which literature indicates are more common in older, overweight, or genetically predisposed animals, not in healthy young adults.[17,18] The choice to use male rats was made to ensure a more controlled experimental environment, as female rats experience hormonal fluctuations that can significantly affect serum metabolites. Studies have shown that male and female rodents exhibit distinct metabolic profiles due to the influence of sex hormones.[19–22] The rats were housed under standard conditions, including a temperature of 25 ± 2°C, humidity maintained at 50–55%, and a 12-hour light/dark cycle. They were provided with free access to standard laboratory feed and water throughout the study. All experimental techniques and procedures were conducted in strict accordance with the ethical guidelines established by the Local Committee of Ethics of Research on Living Creatures in King Saud University Institutional Review Board (ethical reference number: KSU-SE-23-89).

Experimental Protocol

In this study, a total of twenty-four male Sprague-Dawley rats were included and randomly assigned to four experimental groups, with each group comprising six animals. The rationale for using six rats per group is that this study is a toxicity study, and we aimed to minimize the suffering of the animals while ensuring ethical and humane treatment. The experimental groups were structured as follows:

1. Control Group: Received vehicle injection 5% dimethyl sulfoxide (DMSO).
2. VAL Group: Injected with VAL at a dose of 30 mg/kg.
3. DASA Group: Injected with DASA at a dose of 50 mg/kg.
4. Combination Group: Received a combination of VAL (30 mg/kg) and DASA (50 mg/kg).

The doses in this study were chosen based on existing research. VAL was given at 30 mg/kg, which is within the effective range of 20 to 40 mg/kg.[23] DASA was administered at 50 mg/kg, based on its known toxicity in rat studies that tested doses from 30 to 100 mg/kg (FDA Pharmacology/Toxicology Review & Evaluation, NDA 21–986 and 22–072, 2005).[24] Although there are no specific studies on DASA cardiotoxicity, this dose has been linked to liver injury and increased immune cell activity.[25] All treatments were administered intraperitoneally (i.p) every other day for a duration of 14 days. Throughout the study, the body weight of the rats was regularly measured to monitor any changes and assess the overall health and well-being of the animals. At the end of the treatment period, the rats were anesthetized using a ketamine/xylazine mixture administered intraperitoneally at doses of 100 mg/kg and 10 mg/kg, respectively. Following anesthesia, the rats were euthanized by cervical dislocation to ensure a humane and rapid method of sacrifice. Blood and tissue samples were collected from the rats for further analysis and evaluation.

Cardiac Biomarkers Examination

To assess cardiac biomarkers including AST, CPK, and LDH, blood samples were collected from the Sprague-Dawley rats at the end of the treatment period. Blood was drawn via cardiac puncture under anesthesia induced by a ketamine/xylazine mixture. The collected blood samples were allowed to clot and then centrifuged at 1000 ×g for 5 min to separate the serum. The levels of AST, CPK, and LDH in the serum were quantified using reagents obtained from Medical Laboratories Ltd. (Riyadh, Saudi Arabia) according to the manufacturer's instructions.

Histopathological Examination

Heart samples from each experimental group were carefully collected and fixed in 4% neutral buffered formalin for 48 hrs to ensure proper preservation.[26] To prepare the samples for histological analysis, a series of ascending concentrations of ethyl alcohol were used for dehydration. Subsequently, the samples underwent cleaning in xylene, followed by embedding in paraffin at 56°C in a hot oven for 24 hrs. Paraffin blocks were then prepared, and sections with a thickness of 4 µm were cut. The sections were mounted on glass slides and subjected to deparaffinization. To analyze the tissue structure and cellular morphology, the sections were stained with hematoxylin and eosin, allowing for the visualization and examination of various components within the heart tissue. For the assessment of cardiac fibrosis, samples from the left ventricle were fixed in 10% neutral buffered formalin and subsequently embedded in paraffin wax. The paraffin blocks were cut into sections with a thickness of 3 µm. These sections underwent deparaffinization, rehydration, and staining with Masson's trichrome staining, a specific method used to highlight collagen fibers and assess fibrotic changes in the heart tissue.[25] The stained slides were then observed and analyzed using a Nikon Eclipse Ci-L Plus equipped with a Nikon Digital Sight Fi3 camera, allowing for high-resolution imaging and documentation of the histological findings.

Immunohistochemistry Examination

Heart samples were fixed in 4% neutral-buffered formalin and prepared in 4 µm paraffin sections for immunohistochemical analysis. Following deparaffinization and rehydration with xylene and alcohol, the slides underwent blocking with hydrogen peroxide in phosphate-buffered saline (PBS) before being immunoassayed with primary antibodies

targeting p53, p62, BCL-2, and BAX. The incubation with monoclonal antibodies at a 1:50 dilution was carried out overnight at 4°C. Subsequently, the sections were rinsed with PBS and examined using a Nikon Eclipse Ci-L Plus microscope for image capture. To quantify the positive expression of these markers, five random fields were selected from each section, and the positive staining was quantified and plotted in a bar graph.

Sample Preparation for Metabolomics

Serum samples stored at −80°C were thawed to room temperature. A volume of 100 µL of serum was combined with 300 µL of methanol and 100 µL of distilled water in a test tube, followed by vortexing for 2 min. The mixture was then chilled at −20°C for 10 min, centrifuged at 1300 × g at 4°C for 10 min, and 200 µL of the sample supernatant was pipetted into a GC-MS vial and dried under nitrogen gas. Subsequently, a solution of 100 µL methoxyamine hydrochloride in pyridine was added, vortexed for 10 min, and allowed to react for 24 hrs. This was followed by the addition of 100 µL N, O-bis-trimethyl trifluoroacetamide (BSTFA), vortexing for 30 min, and heating the vial at 50°C for 30 min. The processed samples were then ready for analysis using GC-MS.

Metabolomic Profiling

Gas chromatography–mass spectrometry (GC-MS) analysis was performed at the Research Center, College of Pharmacy, King Saud University.[27] Each 1 µL aliquot of derivatized sample was injected into the Perkin Elmer Clarus 600 T gas chromatography equipped with an Elite−5MS capillary column (30 m length, 0.25 µm film thickness, 0.25 mm internal diameter). The temperature program started at 40°C for 2 min, then increased to 150°C at 10°C/min for 2 min, and finally to 300°C at 10°C/min for 2 min. The injector was set to 280°C, and the interface temperature was 250°C. Helium was used as the carrier gas at a flow rate of 1.0 mL/min. Unknown compounds were identified by matching the chromatographic spectra with the National Institute of Standards and Technology (NIST) library and the Wiley 2006 library.

Statistical Analysis

Data analysis and statistical calculations were performed using GraphPad Prism 8 software, presenting the data as mean ± standard deviation (SD). Statistical differences between groups were assessed through analysis of variance (ANOVA) followed by a Tukey-Kramer multiple comparison test. For metabolomics analysis, principal component analysis (PCA) and heatmap visualization were carried out using the MetaboAnalyst web service (https://www.metaboanalyst.ca) with the R statistical package (V.3.6.3). PCA allowed for the exploration of sample clustering and identification of potential patterns or outliers, while the heatmap provided a visual representation of metabolite abundance across different samples. To ensure accurate comparison, the MS peak area for each sample was normalized to the total peak area of all metabolites, with a p-value < 0.05 considered statistically significant, indicating a significant difference between groups.

Results

Assessment of Body Weight and Survival Rate in Rats Treated with VAL ± DASA

Body weight changes were monitored throughout the study period, starting from Day 0 until the conclusion of the experiment. The results indicated no significant difference in body weight between the VAL and VAL + DASA groups compared to the control group (Figure 1A). In contrast, DASA led to a notable decrease in body weight compared to the VAL + DASA group. Additionally, survival rates were assessed over a 14-day monitoring period. At the conclusion of the experiment, no mortality was observed in the VAL and control groups. Conversely, rats treated with DASA exhibited a 50% reduction in survival rate. Notably, the combined treatment of VAL + DASA resulted in no mortality recorded (Figure 1B).

Assessment of Serum CPK, LDH & AST Levels in Rats Treated with VAL ± DASA

The assessment of serum CPK, LDH, and AST levels in rats treated with VAL ± DASA revealed significant insights into cardiac function. Following DASA administration, a significant increase in CPK levels was observed compared to the control group, indicating potential cardiotoxic effects. Conversely, co-administration of VAL with DASA resulted in a significant reduction in

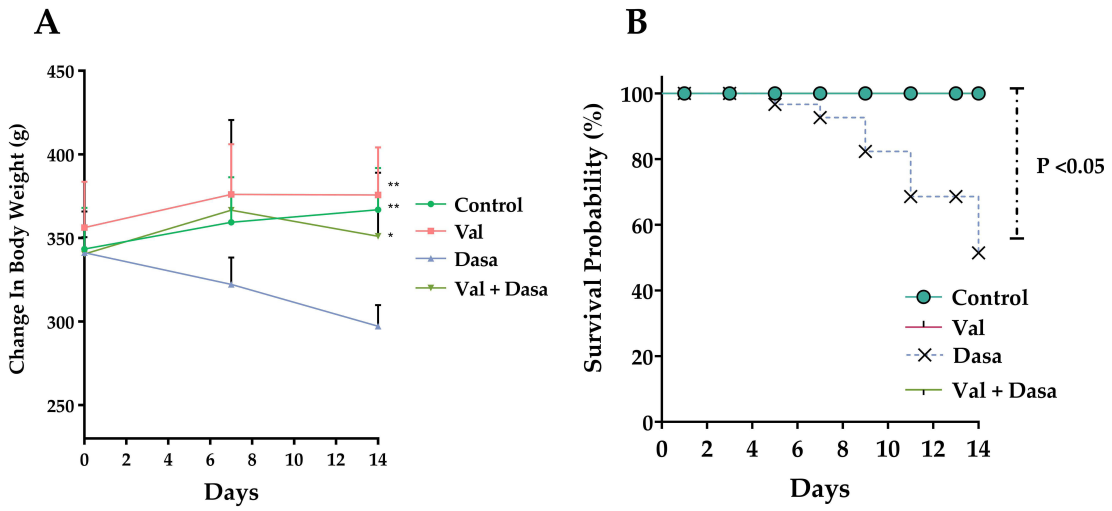

Figure 1 Analysis of Rat Body Weight and Survival in Experimental Groups. (**A**) Monitoring Changes in Rat Body Weight. This graph displays the variations in body weight among rats in the control, VAL, DASA, and VAL + DASA groups over a 14-day period. The body weights of each experimental group are plotted as means ± SD (n = 6). *p<0.05, **p < 0.01 compared to DASA group. (**B**) Survival Rate Analysis in Experimental Groups. The survival rate analysis presents the percentage of surviving rats at each time point throughout the 14-day observation period. The Kaplan-Meier test was used to estimate the survival rate in the different experimental groups. A statistically significant difference in survival probability was observed in the DASA-treated group compared to the group treated with the VAL + DASA combination (p < 0.05).

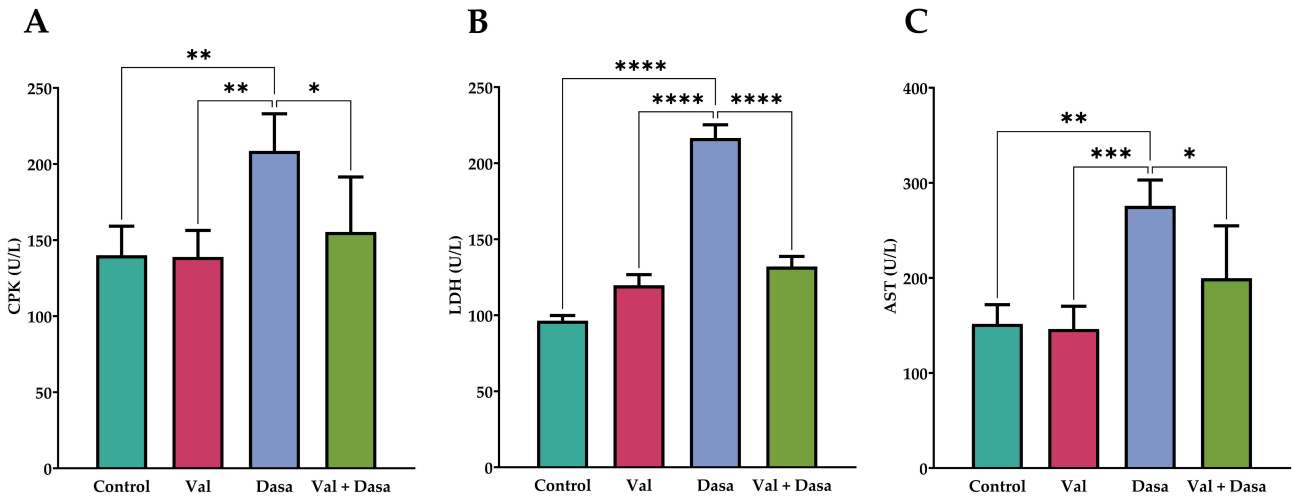

Figure 2 Changes in Serum Cardiac Biomarkers in Rats Treated with VAL ± DASA. (**A**) Creatine Phosphokinase (CPK), (**B**) Lactate Dehydrogenase (LDH), and (**C**) Aspartate Aminotransferase (AST), were analyzed to assess cardiac function. Statistical significance is indicated by asterisks (*p < 0.05, **p < 0.01, ***p < 0.001, ****P<0.0001) compared to the DASA group.

CPK levels (Figure 2A). Similarly, LDH levels, a crucial marker of cardiac injury, were elevated in rats treated with DASA, reflecting cardiac stress. In contrast, the combination of VAL and DASA led to a decrease in LDH levels (Figure 2B). Furthermore, the assessment of AST levels, known for their diagnostic significance in cardiotoxicity, revealed a significant increase after 14 days of DASA administration compared to the control group ($p < 0.01$). Intriguingly, co-treatment with VAL and DASA resulted in a statistically significant decrease in AST level compared to the DASA group, suggesting a potential ameliorative effect on cardiac function (Figure 2C).

Assessment of Cardiac Histopathology in Rats Treated with VAL ± DASA

Histological examination of cardiac tissue sections stained with Hematoxylin and Eosin (H&E) provided valuable insights into the effects of different treatments on cardiac morphology. The control group exhibited normal myocardial tissue architecture without any significant abnormalities (Figure 3A). Similarly, the VAL treated group presented comparable results, indicating that

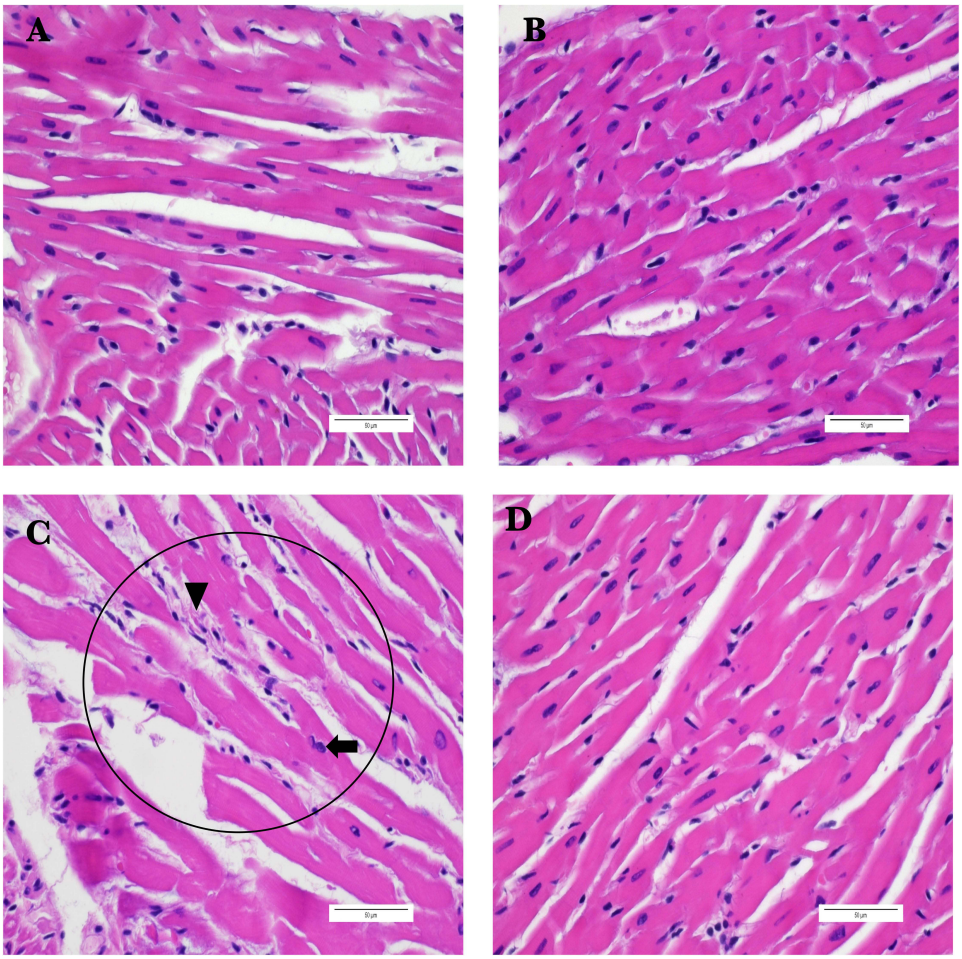

Figure 3 Representative Microscopic Images of H&E-Stained Cardiac Tissue Sections Across Different Experimental Groups. (**A**) Section from the control group showing normal morphology. (**B**) Section from VAL-treated group showing normal morphology. (**C**) Section from DASA-treated group showing chronic inflammation (circles), fibrosis (Arrowhead), and enlarged irregular nuclei (Arrow). (**D**) Section from the DASA+VAL-treated group showing minimal changes in the myocardium. (Scale bar: 50 μm, magnification: ×60).

the tissue architecture was consistent with that of the control group (Figure 3B). In contrast, the group treated with DASA displayed notable histopathological alterations, including enlarged irregular nuclei, fibrosis, inflammation, macrophage infiltration, and signs of myocardial injury such as contraction band necrosis (Figure 3C). Interestingly, the combination treatment of VAL + DASA demonstrated improved cardiac tissue morphology compared to the DASA-treated group. The cardiac tissue in the VAL + DASA group showed minimal changes, suggesting a potential protective effect of the combination therapy on myocardial structure (Figure 3D).

Assessment of Fibrotic Changes in Cardiac Tissue in Rats Treated with VAL ± DASA

The initial H&E staining suggested the presence of fibrotic changes in cardiac tissue, prompting the use of Masson's Trichrome staining to gain a more detailed understanding of these alterations (Figure 4). This approach allowed for a clearer visualization of fibrosis and tissue architecture. In the control and VAL-treated groups, Masson's Trichrome staining revealed no signs of fibrosis, indicating the maintenance of normal cardiac tissue structure (Figure 4A and B). However, the DASA-treated group exhibited evident fibrotic areas (Figure 4C). Additionally, this group showed pronounced contraction band necrosis which was more prominently visualized compared to the H&E staining results. Interestingly, the combination treatment groups displayed only mild fibrotic areas, represented by a light green hue (Figure 4D). This suggests that the presence of both VAL mitigated DASA-induced fibrotic response.

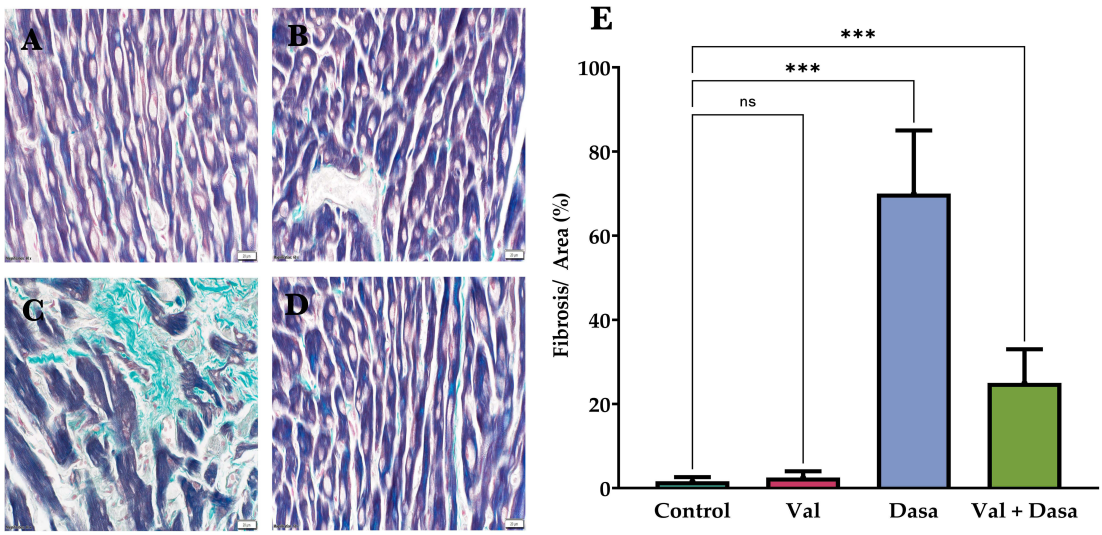

Figure 4 Representative Microscopic Images of Masson's Trichrome-Stained Cardiac Tissue Sections Across Different Experimental Groups. (**A**) Section from the control group showing normal morphology with no signs of fibrosis. (**B**) Section from the VAL-treated group also showing normal morphology without fibrosis. (**C**) Section from the DASA-treated group exhibiting evident fibrotic areas (light green) and pronounced contraction band necrosis (dark green). (**D**) Section from the DASA+VAL-treated group showing only mild fibrotic areas (light green), indicating a mitigated fibrotic response. (**E**) Quantification of fibrosis area over the whole area of five random fields, plotted as bar graphs (Scale bar: 20 μm, magnification: ×40). (ns= non-statistically significant $p>0.05$, ***$p< 0.001$).

Assessment of Cardiac Protein Expression of P53, BAX, BCL-2, and P62 in Rats Treated with VAL ± DASA

Immunohistochemical analysis of cardiac tissue revealed distinct expression patterns of p53, BAX, BCL-2, and P62 across different treatment groups. In the control group, there was no detectable expression of p53, BAX, or P62, while BCL-2 showed moderate expression. The DASA-treated group exhibited significant alterations, with strong positive staining for p53, BAX, and P62, indicating a substantial upregulation of these proteins (Figure 5). Notably, BCL-2 expression was absent in the DASA-treated group. The combination treatment of VAL + DASA resulted in intermediate expression levels, with moderate positive staining for p53, BAX, and P62, suggesting a mitigated response compared to DASA alone. Additionally, BCL-2 expression in the combination group was lower than in the control group but higher than in the DASA-treated group, indicating a partial restoration of BCL-2 levels. These findings suggest that DASA significantly influences the expression of key regulatory proteins involved in apoptosis and autophagy in cardiac tissue, and that the combination treatment with VAL can modulate these effects, potentially offering a protective benefit.

Assessment of Metabolite Profile in Rats Treated with VAL ± DASA

The principal component analysis (PCA) and heat map analysis of the metabolomics data revealed significant insights into the metabolic shifts among the control, VAL, DASA, and VAL + DASA treated groups. As depicted in (Figure 6A), the PCA exhibited a distinct separation pattern for the DASA-treated group, indicating a significant metabolic alteration compared to the other groups. The heat map was utilized to visualize the changes in metabolites among different groups. As shown in (Figure 6B), we analyzed 20 metabolites, and the degree of color in the figure represents the change in metabolite content. Red signifies an increase in the metabolite, while blue indicates a decrease in the metabolite. The results of the heatmap displayed satisfactory clustering, with metabolites in different groups clustered together based on the trends in metabolite changes. To identify potential metabolites, we employed a parameter VIP to reflect the importance of the variables, with each VIP ranked according to its contribution to the classification (Figure 6C).

By applying a selection criterion of VIP > 0.5, 15 metabolites were identified as contributing to the discrimination between the control, VAL, DASA, and VAL + DASA groups. Among the 15 differential metabolites, 5 were upregulated, and 10 were downregulated in the DASA group. Normalized intensities of metabolites revealed significant differences between groups (Figure 7). The notable increase in the levels of 11-eicosaenoic acid, 9-octadecenamide, octadecanoic

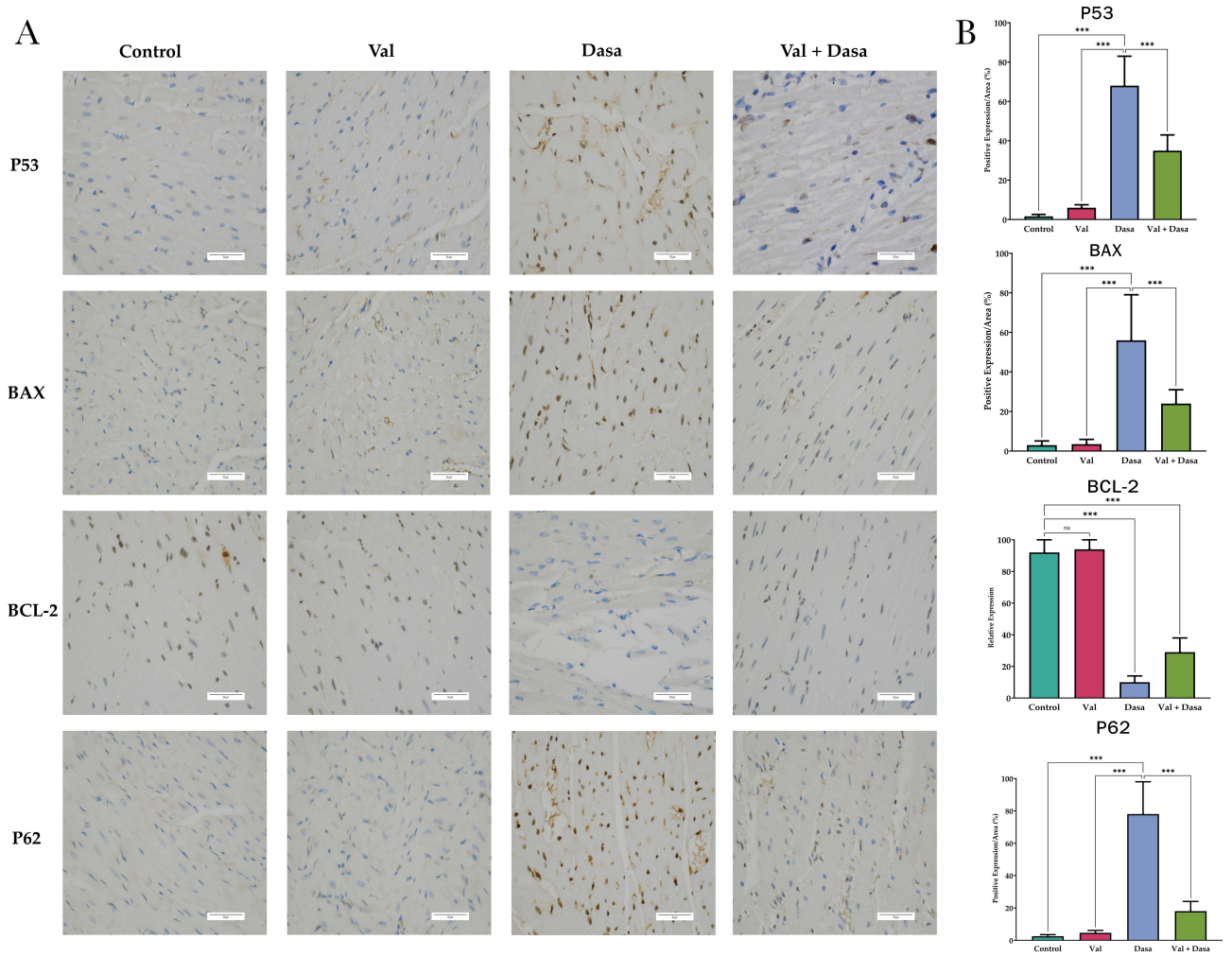

Figure 5 Immunohistochemical Analysis and Quantification of P53, BAX, BCL-2, and P62 Expression in Cardiac Tissue. (**A**) Representative immunohistochemical images showing the expression of P53, BAX, BCL-2 and P62in cardiac tissue sections from different treatment groups. The control group shows no P53, BAX, or P62 expression, with moderate BCL-2 expression. The DASA-treated group exhibits strong P53, BAX, and P62 staining, with no BCL-2 expression. The VAL + DASA combination shows moderate P53, BAX, and P62 staining, with lower BCL-2 expression compared to the control group but higher than the DASA-treated group. (**B**) Bar graph shows P53, BAX, BCL-2, and P62 levels in cardiac tissues across treatments. DASA group exhibits upregulation of P53, BAX, and P62 while downregulation of BCL-2. Combination treatment shows intermediate levels. (ns= non-statistically significant $p>0.05$, ***$p< 0.001$).

acid, and myo-inositol in the DASA group compared to other groups suggests profound alterations in lipid metabolism and inflammation. Conversely, normalized intensities of metabolites indicated that lactic acid was significantly lower in the DASA group than in the control group; however, lactic acid was significantly higher in the VAL group and the combination group compared to DASA. Valine levels were significantly lower in the DASA group than in the control group but significantly higher in the VAL and combination groups compared to DASA. There was a significant decrease in urea levels within the DASA group compared to the control group. In contrast, urea levels were significantly higher in both the VAL and the combination groups compared to the DASA group. Phosphoric acid was significantly lower in the DASA group than in other groups. The level of D-Galactose exhibited a significant reduction in DASA compared to the control. However, in the combination, the level was also reduced to a lesser degree than in DASA. Furthermore, a significant decrease in oleic acid was observed with DASA compared to the control and VAL, while the combination therapy showed a milder decrease compared to DASA.

Overall, the reduction in the levels of oleic acid, D-galactose, phosphoric acid, urea, lactic acid, and L-valine in the DASA group indicates disturbances in energy, carbohydrate, and amino acid metabolism. However, the VAL + DASA combination group mitigates the metabolic disruptions caused by DASA. These findings offer a broad view of the

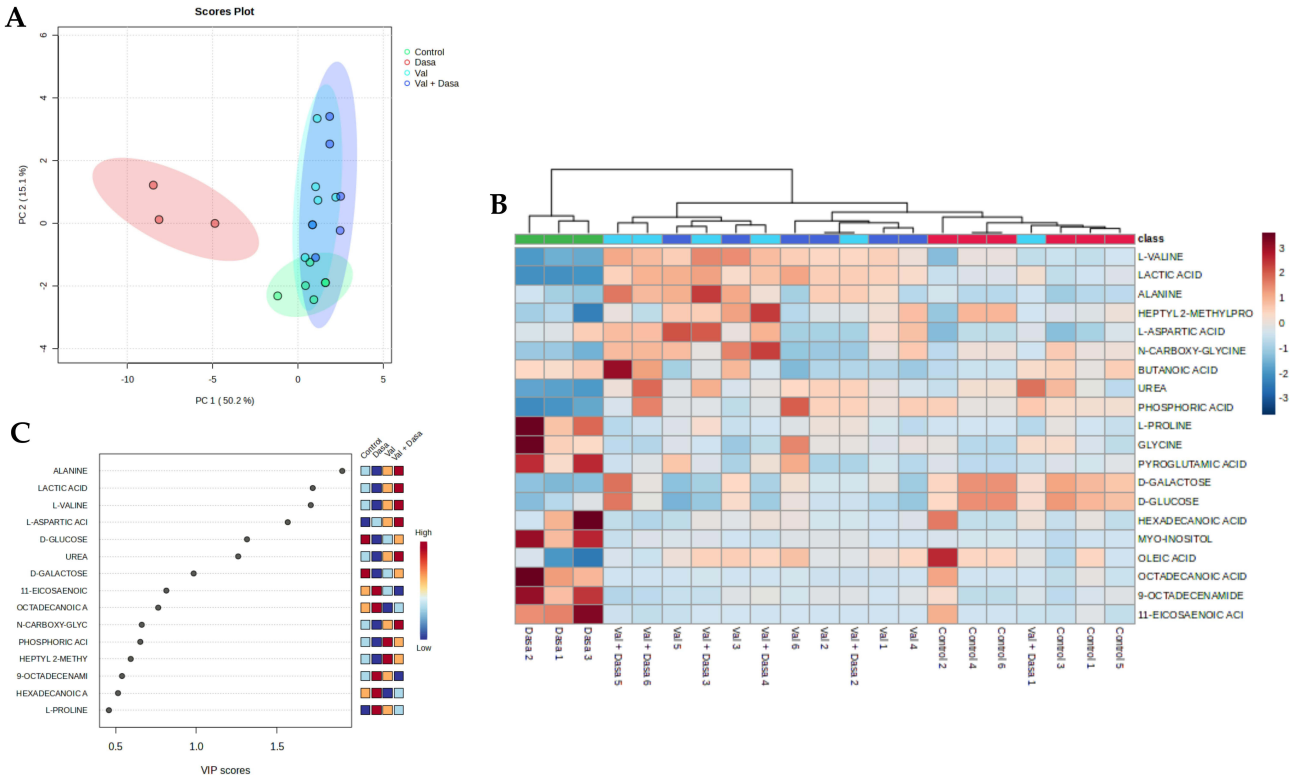

Figure 6 Comprehensive Analysis of Serum Metabolomics. (**A**). Principal Component Analysis (PCA) illustrates the distinct metabolic profiles of the control, DASA, VAL, and VAL + DASA treated groups. Each point represents an individual sample, with the DASA-treated group showing a clear separation from the other groups, indicating a significant shift in metabolic profile. (**B**) Heat map provides a visual representation of the relative levels of metabolites across the control, DASA, VAL, and VAL + DASA treated groups. The color intensity corresponds to the concentration of each metabolite, with the DASA-treated group showing a unique pattern of upregulated and downregulated metabolites. (**C**) VIP scores represent the most contributing metabolites involved in the separation between different groups. This bar chart displays the top 15 upregulated and downregulated metabolites in the DASA-treated group compared to the control, VAL, and VAL + DASA treated groups. The y-axis represents the relative concentration of each metabolite, highlighting the significant metabolic alterations induced by DASA and the potential normalizing effect of VAL.

metabolic changes induced by DASA, highlighting the potential therapeutic role of VAL in managing DASA-induced metabolic alterations.

Discussion

The main objective of this study was to evaluate the potential cardiotoxic effects associated with the administration of Dasatinib, a potent tyrosine kinase inhibitor widely used in cancer treatment. Given the concerns regarding the cardiac safety of Dasatinib, our aim was to investigate its impact on cardiac function and elucidate the underlying mechanisms involved. Furthermore, we aimed to assess the potential protective effects of Valsartan, an angiotensin receptor blocker, against any potential cardiotoxicity induced by Dasatinib. By addressing these objectives, our study aimed to advance the current understanding of the cardiotoxic profile of Dasatinib and explore potential strategies to mitigate any adverse effects on the cardiovascular system.

The results of the study demonstrated a significant reduction in body weights of rats following Dasatinib treatment, indicating potential adverse effects on overall health. This observation is in line with previous clinical trials involving human participants and in vivo studies, where weight loss has been reported as a side effect of Dasatinib treatment.[25,28,29] Intriguingly, when Dasatinib was combined with Valsartan, there was a notable improvement in body weight compared to the use of Dasatinib alone. This suggests that Valsartan could potentially counteract the negative impact of Dasatinib on body weight and mitigate its toxic effects. Moreover, the combination therapy showed promising results by increasing the survival rate of experimental rats that would otherwise subject to the toxic effects of Dasatinib alone. These findings indicate that the combination of Valsartan with Dasatinib may offer a protective effect against Dasatinib-induced toxicity, leading to improved survival outcomes.

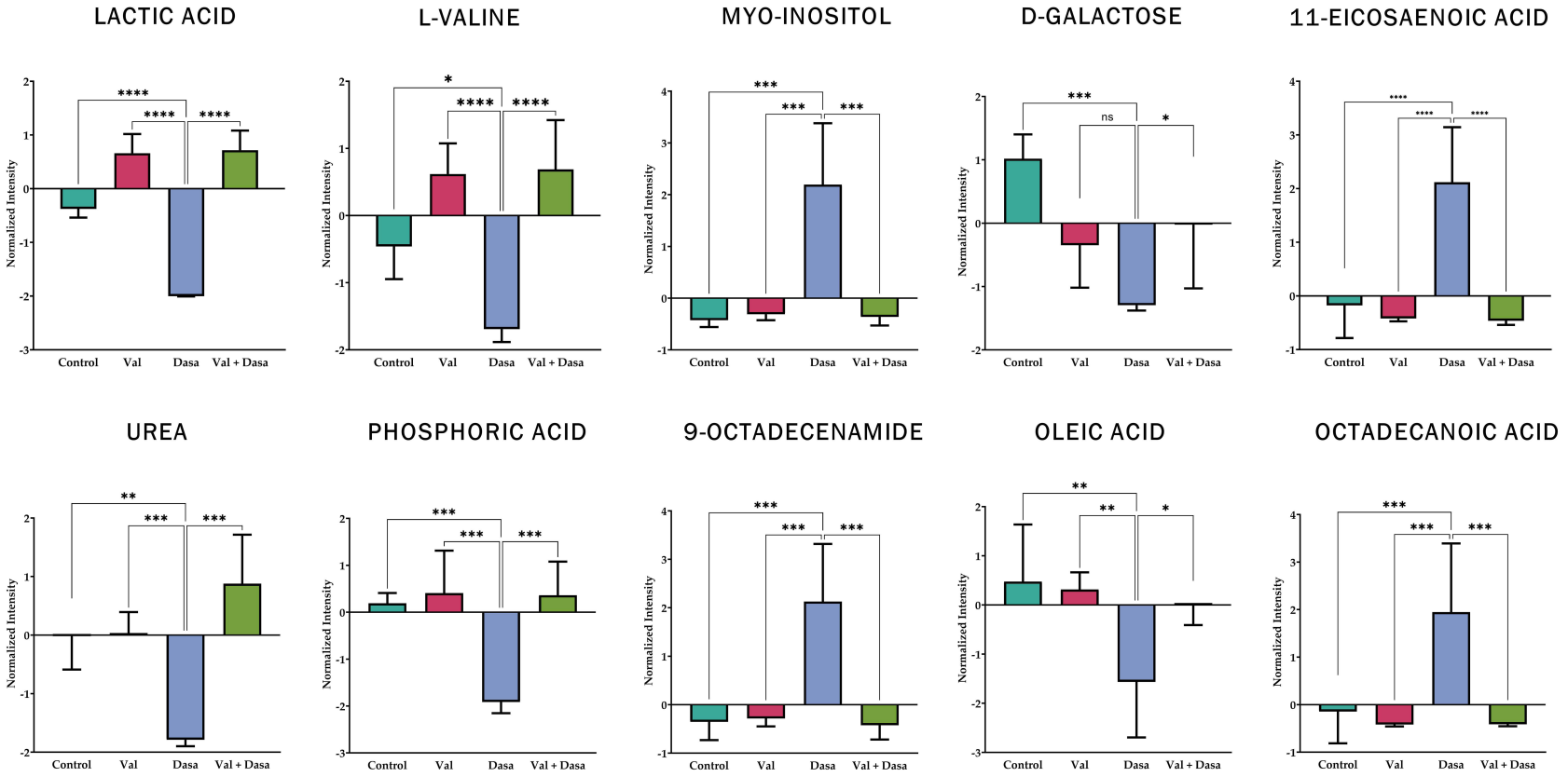

Figure 7 Metabolite Profile Changes in Treatment Groups. The bar graph depicts the normalized intensities of key metabolites across the control, VAL, DASA, and VAL + DASA treated groups, revealing significant differences in metabolic profiles. The data elucidate the distinct impacts of DASA on a range of metabolic pathways involved in lipid metabolism, amino acid metabolism, and energy production. (*p < 0.05, **p < 0.01, ***p< 0.001, ****p<0.0001).

We explored the potential of Valsartan to mitigate Dasatinib-induced cardiotoxicity, with evidence drawn from a range of analyses including histopathological, biochemical, immunohistochemical, and metabolomic analysis. Notably, Dasatinib-treated groups demonstrated a significant increase in AST and CPK compared to the control groups, indicative of myocardial injury.[30,31] Elevated AST levels have been linked to liver injury or myocardial infarction, and higher enzyme activity can lead to significant injuries. Previous studies have reported elevated AST levels in patients with chronic myeloid leukemia who were treated with Dasatinib, with one study showing that 111 out of 186 patients exhibited increased AST levels after 8 months of treatment.[32] Additionally, there was a case where a patient in the Dasatinib group had to discontinue treatment due to elevated creatine phosphokinase levels.[33] These findings support our observations that Dasatinib treatment can lead to elevated levels of these enzymes, indicating potential myocardial injury. However, our study demonstrated that the introduction of Valsartan treatment in Dasatinib-treated groups resulted in a reduction of these marker enzymes, suggesting a protective effect of Valsartan against Dasatinib-induced myocardial injury in rats. The decrease in AST and CPK levels in the combination therapy group aligns with previous research findings,[34,35] further supporting the notion that Valsartan may mitigate the cardiotoxic effects of Dasatinib.

The histopathological analysis of cardiac tissue obtained from Dasatinib-treated rats revealed significant signs of chronic myocardial infarction, fibrosis, and necrosis of the contraction band, indicating the detrimental effects of Dasatinib on cardiac tissue. However, when Valsartan was combined with Dasatinib, these observations were minimal, suggesting that Valsartan may have a protective effect against the histopathological changes induced by Dasatinib in the heart. The reduction in chronic myocardial infarction, fibrosis, and necrosis of the contraction band in the combination treatment group highlights the potential of Valsartan in mitigating the adverse effects of Dasatinib on cardiac tissue. Our study, in line with previous research, emphasizes the role of over-activation of apoptosis in decreasing the number of myocardial cells, leading to cardiac dysfunction.[36] We found that Dasatinib significantly decreased BCL-2 and enhanced the expression of BAX genes, indicating a significant contribution of treatment-induced cardiac toxicity to apoptosis. This finding is supported by Hasinoff & Patel (2020),[6] who revealed that Dasatinib induced apoptosis in myocytes by increasing the activity of caspase 3/7 and lactate dehydrogenase. They also found that treating myocytes with 2-M Dasatinib for three hours slightly increased the levels of BAX protein, altered mitochondrial permeability, and induced apoptosis. In contrast, rats treated with DASA and Valsartan showed a significant decrease in BAX and an increase in BCL-2, suggesting that Valsartan protects against DASA-induced cardiotoxicity. This aligns with previous studies demonstrating the cardioprotective properties of Valsartan against apoptosis in various heart diseases.[11,37] Furthermore, we found that DASA activated apoptosis by upregulating the protein expression of p53, a tumor suppressor protein known to promote apoptosis. Similar results were reported with sorafenib and gefitinib, other tyrosine kinase inhibitors, which induced cardiomyocyte apoptosis by increasing p53 expression.[38–40] However, the combination treatment of DASA with Valsartan significantly reduced p53 expression, consistent with the findings of Wu et al,[41] who showed the protective role of Valsartan against cardiomyocyte apoptosis through the inhibition of the CHOP/Puma signaling pathway.

The observed changes in serum metabolomics data provide a potential understanding of the cardiotoxic effects of Dasatinib and the protective role of Valsartan. The significant increase in the levels of 11-eicosanenoic acid, 9-octadecenamide, octadecanoic acid, myo-inositol, and glycine in the Dasatinib-treated group suggests profound alterations in lipid metabolism, inflammation, and cellular stress response. These increases could be indicative of an inflammatory response triggered by Dasatinib, leading to oxidative stress and subsequent cardiac damage. Conversely, the reduction in the levels of oleic acid, D-galactose, phosphoric acid, urea, lactic acid, and L-valine in the Dasatinib-treated group indicates disturbances in energy metabolism, carbohydrate metabolism, and amino acid metabolism. Valsartan's protective effects may be attributed to its ability to modulate the renin-angiotensin-aldosterone system (RAAS) and inhibit the angiotensin II receptor. This modulation likely explains the observed normalization of metabolite levels in the combination of Valsartan and Dasatinib-treated groups, indicating a protective effect against Dasatinib-induced cardiotoxicity. In conclusion, the altered levels of metabolites associated with lipid metabolism, inflammation, cellular stress response, energy metabolism, and amino acid metabolism suggest the cardiotoxic effects of Dasatinib in Sprague Dawley rats. The protective effects of Valsartan are likely mediated through its ability to modulate the RAAS and mitigate the detrimental

effects of Dasatinib on cardiac function. Further studies are warranted to elucidate the underlying mechanisms and validate these findings.

While serum metabolomics data provides valuable insights into the cardiotoxic effects of Dasatinib, it is important to acknowledge several limitations of using this data alone to infer cardiotoxicity. One significant limitation is that Dasatinib can induce systemic toxicity in other organs, such as the liver and kidneys, which may alter serum metabolite levels. Since these organs play crucial roles in metabolite processing and elimination, any impairment in their function due to Dasatinib toxicity could confound the interpretation of serum metabolite changes, making it difficult to attribute these alterations directly to cardiotoxic effects. Additionally, the small sample size, with only six rats per group, limits the statistical power and reliability of the findings. To gain a more comprehensive understanding of the cardiotoxicity of Dasatinib, it would be beneficial to complement serum metabolomics data with histopathological examination of the heart, liver, and kidneys, as well as functional assessments of cardiac parameters. Furthermore, conducting oxidative stress and inflammation assessments during this study would provide critical insights, as these parameters are well-known indicators of cardiotoxicity. This multi-faceted approach would provide a more accurate assessment of the cardiotoxic effects of Dasatinib and help elucidate the underlying mechanisms involved. By examining the histological changes in the heart, liver, and kidneys, we can directly observe any structural damage or abnormalities caused by Dasatinib. Additionally, assessing cardiac parameters such as electrocardiogram (ECG) readings, heart rate, and blood pressure can provide insights into the functional impact of Dasatinib on the cardiovascular system. Integrating these different aspects of analysis, including oxidative stress and inflammation parameters, will enable us to obtain a more comprehensive understanding of the cardiotoxic effects of Dasatinib and differentiate them from potential systemic toxicities. This approach will contribute to a more accurate assessment of the drug's safety profile and aid in the development of strategies to mitigate its adverse effects. These findings highlight the potential benefits of combining Valsartan with Dasatinib in mitigating adverse effects and improving overall health outcomes. Further research is warranted to elucidate the underlying mechanisms responsible for these observed effects and to optimize the dosing regimens for this combination therapy.

Conclusion

This study reveals that Dasatinib induces cardiotoxicity, as evidenced by damage to cardiac tissue. The combination with Valsartan significantly reduces these detrimental effects, suggesting a cardioprotective role for Valsartan. These findings highlight the potential of combination therapies to mitigate cardiotoxicity associated with anticancer treatments. Further research is needed to elucidate the underlying mechanisms and assess the clinical relevance of this combination for improving patient outcomes.

Ethical Approval

This animal study involving Sprague-Dawley (SD) rats was conducted in compliance with the ethical standards and guidelines established by the Research Ethics Committee (REC) at King Saud University. The project received formal approval with ethics reference number KSU-SE-23-89.

Acknowledgment

The authors would like to express their sincere gratitude to the Researchers Supporting Project for the financial support through grant number RSPD2024R593.

Funding

This research was funded by the Researchers Supporting Project number RSPD2024R593, King Saud University, Riyadh, Saudi Arabia.

Disclosure

The authors declare no competing interests in this work.

References

1. Daher IN, Daigle TR, Bhatia N, Durand JB. The prevention of cardiovascular disease in cancer survivors. *Tex Heart Inst J*. 2012;39(2):190–198.
2. Higgins AY, O'Halloran TD, Chang JD. Chemotherapy-induced cardiomyopathy. *Heart Fail Rev*. 2015;20(6):721–730. doi:10.1007/s10741-015-9502-y
3. Chen MH, Kerkelä R, Force T. Mechanisms of cardiac dysfunction associated with tyrosine kinase inhibitor cancer therapeutics. *Circulation*. 2008;118(1):84–95. doi:10.1161/CIRCULATIONAHA.108.776831
4. Talpaz M, Shah NP, Kantarjian H, et al. Dasatinib in imatinib-resistant Philadelphia chromosome–positive leukemias. *N Engl J Med*. 2006;354(24):2531–2541. doi:10.1056/NEJMoa055229
5. Ottmann O, Dombret H, Martinelli G, et al. Dasatinib induces rapid hematologic and cytogenetic responses in adult patients with Philadelphia chromosome–positive acute lymphoblastic leukemia with resistance or intolerance to imatinib: interim results of a Phase 2 study. *Blood*. 2007;110(7):2309–2315. doi:10.1182/blood-2007-02-073528
6. Hasinoff BB, Patel D. Mechanisms of the cardiac myocyte-damaging effects of dasatinib. *Cardiovasc Toxicol*. 2020;20(4):380–389. doi:10.1007/s12012-020-09565-7
7. Chaar M, Kamta J, Ait-Oudhia S. Mechanisms, monitoring, and management of tyrosine kinase inhibitors-associated cardiovascular toxicities. *Onco Targets Ther*. 2018;11:6227–6237. doi:10.2147/OTT.S170138
8. Jung KH, Chu K, Lee ST, et al. Blockade of AT1 receptor reduces apoptosis, inflammation, and oxidative stress in normotensive rats with intracerebral hemorrhage. *J Pharmacol Exp Ther*. 2007;322(3):1051–1058. doi:10.1124/jpet.107.120097
9. Alanazi WA, Alhamami HN, Alshamrani AA, et al. Valsartan prevents gefitinib-induced lung inflammation, oxidative stress, and alteration of plasma metabolites in rats. *Saudi J Biol Sci*. 2023;30(2):103522. doi:10.1016/j.sjbs.2022.103522
10. Al-Hamadi A, Al-Sabri N, Aldujele IB, Al-Fatlawi AJ, Allebban Z S. Valsartan attenuates cardiotoxicity in breast cancer patients after chemotherapy. *J Cancer Sci Ther*. 2018;10(05). doi:10.4172/1948-5956.1000526
11. Sakr HF, Abbas AM, Elsamanoudy AZ. Effect of valsartan on cardiac senescence and apoptosis in a rat model of cardiotoxicity. *Can J Physiol Pharmacol*. 2016;94(6):588–598. doi:10.1139/cjpp-2015-0461
12. Chen DQ, Chen H, Chen L, Tang DD, Miao H, Zhao YY. Metabolomic application in toxicity evaluation and toxicological biomarker identification of natural product. *Chem Biol Interact*. 2016;252:114–130. doi:10.1016/j.cbi.2016.03.028
13. Yan SK, Liu RH, Jin HZ, et al. "Omics" in pharmaceutical research: overview, applications, challenges, and future perspectives. *Chin J Nat Med*. 2015;13(1):3–21. doi:10.1016/S1875-5364(15)60002-4
14. Vinaixa M, Schymanski EL, Neumann S, Navarro M, Salek RM, Yanes O. Mass spectral databases for LC/MS- and GC/MS-based metabolomics: state of the field and future prospects. *TrAC Trends in Analytical Chemistry*. 2016;78:23–35. doi:10.1016/j.trac.2015.09.005
15. Robertson DG. Metabonomics in Toxicology: a Review. *Toxicol Sci*. 2005;85(2):809–822. doi:10.1093/toxsci/kfi102
16. Brower M, Grace M, Kotz CM, Koya V. Comparative analysis of growth characteristics of Sprague Dawley rats obtained from different sources. *Lab Anim Res*. 2015;31(4):166. doi:10.5625/lar.2015.31.4.166
17. Luo X, Yu W, Liu Z, et al. Ageing increases cardiac electrical remodelling in rats and mice via NOX4/ROS/CaMKII-mediated calcium signalling. *Oxid Med Cell Longev*. 2022;2022:1–15. doi:10.1155/2022/8538296
18. Capitanio D, Leone R, Fania C, Torretta E, Gelfi C. Sprague Dawley rats: a model of successful heart aging. *EuPA Open Proteom*. 2016;12:22–30. doi:10.1016/j.euprot.2016.03.017
19. Novelle MG, Vázquez MJ, Peinado JR, et al. Sequential exposure to obesogenic factors in females rats: from physiological changes to lipid metabolism in liver and mesenteric adipose tissue. *Sci Rep*. 2017;7(1):46194. doi:10.1038/srep46194
20. Quirós Cognuck S, Reis WL, Silva M, et al. Sex differences in body composition, metabolism-related hormones, and energy homeostasis during aging in Wistar rats. *Physiol Rep*. 2020;8(20). doi:10.14814/phy2.14597
21. Liang Q, Xu W, Hong Q, et al. Rapid comparison of metabolites in humans and rats of different sexes using untargeted ultraperformance liquid chromatography coupled to time-of-flight mass spectrometry and an in-house software platform. *Eur J Mass Spectrom*. 2015;21(6):801–821. doi:10.1255/ejms.1395
22. Ruoppolo M, Caterino M, Albano L, et al. Targeted metabolomic profiling in rat tissues reveals sex differences. *Sci Rep*. 2018;8(1):4663. doi:10.1038/s41598-018-22869-7
23. Wilkinsonberka J, G TAN, JAWORSKI K, NINKOVIC S. Valsartan but not atenolol improves vascular pathology in diabetic Ren-2 Rat retina. *Am J Hypertens*. 2007;20(4):423–430. doi:10.1016/j.amjhyper.2006.09.018
24. Hastings K Pharmacology Reviews. June 28, 2006. Available from: https://www.accessdata.fda.gov/drugsatfda_docs/nda/2006/021986s000_Sprycel__PharmR.pdf. Accessed November 22, 2024.
25. Alhazzani K, Alrewily SQ, Aljerian K, et al. Hydroxychloroquine ameliorates dasatinib-induced liver injury via decrease in hepatic lymphocytes infiltration. *Hum Exp Toxicol*. 2023;42. doi:10.1177/09603271231188492
26. Alanazi AZ, Alqinyah M, Alhamed AS, et al. Cardioprotective effects of liposomal resveratrol in diabetic rats: unveiling antioxidant and anti-inflammatory benefits. *Redox Rep*. 2024;29(1):2416835. doi:10.1080/13510002.2024.2416835
27. Assiri MA, Al Jumayi SR, Alsuhaymi S, et al. Electronic cigarette vapor disrupts key metabolic pathways in human lung epithelial cells. *Saudi Pharm J*. 2024;32(1):101897. doi:10.1016/j.jsps.2023.101897
28. Sillaber C, Herrmann H, Bennett K, et al. Immunosuppression and atypical infections in CML patients treated with dasatinib at 140 mg daily. *Eur J Clin Invest*. 2009;39(12):1098–1109. doi:10.1111/j.1365-2362.2009.02206.x
29. Xue T, Luo P, Zhu H, et al. Oxidative stress is involved in Dasatinib-induced apoptosis in rat primary hepatocytes. *Toxicol Appl Pharmacol*. 2012;261(3):280–291. doi:10.1016/j.taap.2012.04.010
30. Shanmugara TS, Arunsundar M, Somasundar I, Krishnakum E, Sivaraman D, Ravichandi V. Cardioprotective effect of ficus hispida linn. on cyclophosphamide provoked oxidative myocardial injury in a rat model. *Int J Pharm*. 2008;4(2):78–87. doi:10.3923/ijp.2008.78.87
31. Swanson JR, Wilkinson JH, Conn RB, Hess JW, Natho GJW. Measurement of Creatine kinase activity in serum. In: *Standard Methods of Clinical Chemistry*; 1972:33–42. doi:10.1016/B978-0-12-609107-6.50011-8
32. Hochhaus A, Kantarjian HM, Baccarani M, et al. Dasatinib induces notable hematologic and cytogenetic responses in chronic-phase chronic myeloid leukemia after failure of imatinib therapy. *Blood*. 2007;109(6):2303–2309. doi:10.1182/blood-2006-09-047266

33. Kantarjian H, Shah NP, Hochhaus A, et al. Dasatinib versus imatinib in newly diagnosed chronic-phase chronic myeloid leukemia. *N Engl J Med*. 2010;362(24):2260–2270. doi:10.1056/NEJMoa1002315
34. Alhazzani K, Alotaibi MR, Alotaibi FN, et al. Protective effect of valsartan against doxorubicin-induced cardiotoxicity: histopathology and metabolomics in vivo study. *J Biochem Mol Toxicol*. 2021;35(9). doi:10.1002/jbt.22842
35. Keles MS, Bayir Y, Suleyman H, Halici Z. Investigation of effects of Lacidipine, Ramipril and Valsartan on DNA damage and oxidative stress occurred in acute and chronic periods following isoproterenol-induced myocardial infarct in rats. *Mol Cell Biochem*. 2009;328(1–2):109–117. doi:10.1007/s11010-009-0080-y
36. Bennett MR. Apoptosis in the cardiovascular system: incidence, regulation, and therapeutic options. In: *Apoptosis in Health and Disease*. Cambridge University Press; 2005:156–187. doi:10.1017/CBO9780511663543.006
37. Hadi Najah R, Al-Amran Fhadil G, Hussien Yasmeem A, Al-Yasiri Israa K, Al-Turfy M. Experimental immunology The cardioprotective potential of valsartan in myocardial ischaemia reperfusion injury. *Cent Eur J Immunol*. 2015;2:159–166. doi:10.5114/ceji.2015.52829
38. Grabowska ME, Chun B, Moya R, Saucerman JJ. Computational model of cardiomyocyte apoptosis identifies mechanisms of tyrosine kinase inhibitor-induced cardiotoxicity. *J Mol Cell Cardiol*. 2021;155:66–77. doi:10.1016/j.yjmcc.2021.02.014
39. Korashy HM, Attafi IM, Ansari MA, et al. Molecular mechanisms of cardiotoxicity of gefitinib in vivo and in vitro rat cardiomyocyte: role of apoptosis and oxidative stress. *Toxicol Lett*. 2016;252:50–61. doi:10.1016/j.toxlet.2016.04.011
40. Yang Q, Zhang C, Wei H, et al. Caspase-independent pathway is related to nilotinib cytotoxicity in cultured cardiomyocytes. *Cell Physiol Biochem*. 2017;42(6):2182–2193. doi:10.1159/000479993
41. Wu T, Dong Z, Geng J, et al. Valsartan protects against ER stress-induced myocardial apoptosis via CHOP/Puma signaling pathway in streptozotocin-induced diabetic rats. *Eur J Pharm Sci*. 2011;42(5):496–502. doi:10.1016/j.ejps.2011.02.005